

CONJUGATE HEAT TRANSFER ANALYSIS IN CRYOGENIC MICROCHANNEL HEAT EXCHANGER

A THESIS SUBMITTED IN PARTIAL FULFILLMENT OF THE
REQUIREMENTS FOR THE DEGREE OF

**Master of Technology
in
Mechanical Engineering**

By

Rasmikanti Biswal



**Department of Mechanical Engineering
National Institute of Technology Rourkela
Rourkela 769008**

June 2015

CONJUGATE HEAT TRANSFER ANALYSIS IN CRYOGENIC MICROCHANNEL HEAT EXCHANGER

A THESIS SUBMITTED IN PARTIAL FULFILLMENT OF THE
REQUIREMENTS FOR THE DEGREE OF

**Master of Technology
in
Mechanical Engineering**

By

Rasmikanti Biswal

Under the Guidance of
Dr. Manoj Kumar Moharana



**Department of Mechanical Engineering
National Institute of Technology Rourkela
Rourkela 769008**

June 2015



National Institute of Technology Rourkela

Rourkela 769008

CERTIFICATE

This is to certify that the thesis entitled **“CONJUGATE HEAT TRANSFER ANALYSIS IN CRYOGENIC MICROCHANNEL HEAT EXCHANGER”** submitted to the National Institute of Technology Rourkela by **Rasmikanti Biswal**, Roll No. 213ME5443 for the award of the Degree of **Master of Technology in Mechanical Engineering** with specialization in **Cryogenic and Vacuum Technology** is a record of bonafide research work carried out by her under my supervision and guidance.

To the best of my knowledge, the matter embodied in this thesis has not been submitted to any other University or Institute for the award of any degree or diploma.

Dr. Manoj Kumar Moharana

Assistant Professor

Department of Mechanical Engineering
National Institute of Technology Rourkela

Place: Rourkela

Date: **01 / June / 2015**

SELF DECLARATION

I, **Rasmikanti Biswal**, Roll No. - **213ME5443**, student of M. Tech (2013-2015), Cryogenic and Vacuum Technology at Department of Mechanical Engineering, National Institute of Technology, Rourkela do here by declare that I have not adopted any kind of unfair means and carried out the research work reported in this thesis ethically to the best of my knowledge. If adoption of any kind of unfair means is found in this thesis work at a later stage, then appropriate action can be taken against me including withdrawal of this thesis work.

NIT, ROURKELA
DATE: 01-06-2015

Rasmikanti Biswal
Rasmikanti Biswal

ACKNOWLEDGEMENT

I am extremely fortunate to be involved in an exciting and challenging research project like **“CONJUGATE HEAT TRANSFER ANALYSIS IN CRYOGENIC MICROCHANNEL HEAT EXCHANGER”**. It has enriched my life, giving me an opportunity to work in a new environment of Cryogenic heat transfer. This project increased my thinking and understanding capability and after the completion of this project, I experience the feeling of achievement and satisfaction.

I would like to express my greatest gratitude and respect to my supervisor **Dr. Manoj Kumar Moharana**, for his excellent guidance, valuable suggestions. He has been not only a wonderful supervisor but also a genuine person. I consider myself extremely lucky to be able to work under the guidance of such a dynamic personality.

I also express my special thanks to **Prof. Ashok Kumar Satpathy**, who has provided CFD Lab where I have completed maximum part of my project work and thanks to my classmate for their support during my project work. I would like to express my thanks to all staffs and faculty members of the mechanical engineering department for making my stay in N.I.T. Rourkela a pleasant and memorable experience and also giving me absolute working environment.

Last but not the least; I want to convey my heartiest gratitude to my parents for their immeasurable love, support and encouragement.

DATE: 01/June/2015

Rasmikanti Biswal
Rasmikanti Biswal
Roll No. 213ME5443
Cryogenic and Vacuum Technology

ABSTRACT

Printed circuit heat exchanger (PCHE) is a highly integrated plate type compact heat exchanger and most important as well as a most critical component in the cryogenic application. Compact heat exchangers are characterized by area density ($\beta = A_{HT} / V$) i.e. heat transfer area per unit volume of the heat exchanger. The area density of compact heat exchanger is $\geq 700 \text{ m}^2/\text{m}^3$ where the area density of printed circuit heat exchanger is $\geq 25000 \text{ m}^2/\text{m}^3$. Printed circuit heat exchangers are highly compact compared to conventional heat exchangers. The hydraulic diameter is less than 1mm. Printed Circuit Heat Exchanger manufacturing process is followed by chemical etching and chemical bonding. Microchannels for fluid flow are constructed by chemical etching of the metal plates according to different configuration then plates are stacked alternately and assembled by diffusion bonding. Due to its compact size, high efficiency, large heat transfer area PCHE (microchannel heat exchanger) are used in cryogenic refrigeration and liquefaction systems.

A counter flow rectangular microchannel (40 mm \times 1.6 mm \times 1.2 mm) printed circuit heat exchanger is designed and simulated using commercial ANSYS FLUENT. The performance is investigated numerically with helium at cryogenic temperature. The performance is affected by axial conduction at low Reynolds number ($Re \leq 100$). Because of length and viscous nature, the fluid flow through the channel is laminar and thermally fully developed.

The Nusselt number (Nu), flux, dimensionless fluid temperature and wall temperature, effectiveness are determined for different Reynolds number Reynolds number ($Re \leq 100$) with varying material i.e. wall to fluid thermal conductivity ratio ($k_{sf} = 141.58 - 5061.5$). Axial conduction (λ) is calculated by using Kroeger's equation. Effectiveness is calculated to investigate the thermal performance of the microchannel heat exchanger.

Keywords: PCHE, microchannel, axial conduction, effectiveness, Reynolds number, Nusselt number

CONTENTS

CERTIFICATE	i
ACKNOWLEDGEMENT	ii
ABSTRACT	iii
CONTENTS	iv
LIST OF FIGURES	vi
LIST OF TABLES	vii
NOMENCLATURE	viii
Chapter1	1
Introduction	1
1.1. Printed Circuit Heat Exchanger (HEATRIC™ Type)	1
1.1.1. Advantages of PCHE:	2
1.1.2. Disadvantages of PCHE:	2
1.1.3. Materials Selection	3
1.1.4. Manufacturing	3
1.1.5. Design of Printed Circuit Heat Exchanger (HEATRIC™ type)	4
1.1.6. Applications	7
1.2. Axial conduction	8
1.3. Objectives of the thesis	10
1.4. Organization of thesis	10
Chapter 2	11
Literature review	11
2.1 Microchannel	11
2.2 Printed circuit heat exchanger	13
Chapter 3	15
Numerical simulation	15
3.1 Introduction	15
3.2 Governing equations	15
3.3 Selection of materials	16
3.4 Thermo-physical properties of cryogenic fluid	17
3.5 Grid independence test.	17

3.6 Computational domain and boundary condition	18
3.7 Mathematical Modelling	19
3.8 Solution approaches	20
Chapter 4	21
Results and discussion	21
Chapter 5	27
Conclusion	27
References	28

LIST OF FIGURES

Figure No.	Description	Page No.
1.1	Step 1. Plate passage	4
1.2	Step 2. Diffusion bonding of plates	5
1.3	Step 3. A blocked composed of diffusion bonded plates	5
1.4	Step 3 welding of nozzles and header to HX	6
1.5	The final Product	6
1.6	Simple cross flow (left) and cross flow (right) configuration	7
1.7	Axial variation of bulk fluid and local wall temperature along the flow direction of a circular duct subjected to (a) constant wall heat flux (b) constant wall temperature	9
3.1	Computational domain and geometry of micro channel heat exchanger	17
4.1	Variation of fluid temperature along the length of microchannel heat exchanger as a function of Re and k_{sf} (a-b) hot channel (c-d) cold channel.	20
4.2	Variation of wall temperature along the length of microchannel heat exchanger as a function of Re and k_{sf} (a-b) hot channel (c-d) cold channel.	21
4.3	Variation of dimensionless fluid and wall temperature along the length of microchannel heat exchanger as a function of Re and k_{sf} (a-b) hot channel (c-d) cold channel	22
4.4	Variation of heat flux along the length of microchannel heat exchanger as a function of Re and k_{sf} (a-b) hot channel (c-d) cold channel	23
4.5	Variation of Nusselt number along the length of microchannel heat exchanger as a function of Re and k_{sf} (a-b) hot channel (c-d) cold channel	24
4.6	Variation of axial conduction of the microchannel heat exchanger with variation of Re as a function k_{sf}	25
4.7	Thermal performance of microchannel heat exchanger (ϵ) with variation of Re as a function of k_{sf}	25

LIST OF TABLES

Table No.	Description	Page No.
3.1	List of Materials used for the microchannel	16
3.2	Boundary conditions	17
3.3	Velocity at Reynolds number 50	18
3.4	Velocity at Reynolds number 80	18

NOMENCLATURE

A	Heat transfer area
A_{cs}	Cross-sectional area
A_{HT}	Heat transfer area
A_w	Cross-sectional area of wall
C_v	Specific heat at constant volume
C_{min}	Minimum specific heat
D_h	Hydraulic diameter
H	Channel depth
h	Heat transfer coefficient, W/m^2K
k_s	Thermal conductivity of solid
k_f	Thermal conductivity of fluid
k_{sf}	Thermal conductivity ratio solid to fluid
L	Length of microchannel heat exchanger
\dot{m}	Mass flow rate, kg/s
Nu	Nusselt number
P	Pressure, Pa
P	Perimeter
q''	Heat flux
Q	Heat transfer
Q_{actual}	Actual heat transfer
Q_{max}	Actual heat transfer
Re	Reynolds number
T_w	Temperature of wall
T_f	Temperature of fluid
$T_{hot, in}$	Temperature of hot fluid at inlet
$T_{cold, in}$	Temperature of cold fluid at inlet
$T_{hot, out}$	Temperature of hot fluid at outlet
$T_{cold, out}$	Temperature of cold fluid at outlet
V_f	Velocity, m/sec

V	Volume, m^3
W	Channel width
Z^*	Length of channel in dimensionless form

Greek Symbols

ε	Effectiveness
λ	Dimensionless axial conduction parameter
μ	Dynamic viscosity
ρ	Density
Θ	Non-dimensional Temperature
β	Area density

Abbreviations

PCHE	Printed Circuit Heat Exchanger
------	--------------------------------

CHAPTER 1

Introduction

A heat exchanger is a mechanical device that transfers heat or thermal energy between two or more fluids at the different temperature. There is no work and heat interaction in a heat exchanger. Heat flow is a function of the temperature difference between the fluids, area of the heat interaction and the convective or conductive property of the fluid. This formula is invented by Newton known as Newton's law of cooling that is given by

$$Q = hA\Delta T \quad (1.1)$$

where h is the heat transfer coefficient (W/m^2K), A is heat transfer area (m^2), and ΔT is the temperature difference (K).

For cryogenic application heat exchangers are classified into two categories according to operating pressure, operation and investment cost, flow rate, heavy duty and compactness (high area density). (1) Recuperators and (2) Regenerator

Recuperators: In recuperators heat is transferred from the hot fluid to the cold fluid by means of a separator (separating wall) no direct mixing of fluids. Fluid moves in separate fluid microchannels have no moving parts. Heat transfer takes place from some boundary condition under steady state. Example: tubular, plate-fin, perforated plate.

Regenerator: Regenerator consists of a matrix through which hot stream and cold stream flows alternately and periodically. Hot fluid gives up the heat to the generator and cold fluid passing through the same passage picks up the stored heat. Heat transfer is transient i.e. depends on position and time.

1.1. Printed Circuit Heat Exchanger (HEATRIC™ Type)

Printed Circuit Heat exchanger is a sort plate type compact heat exchanger was invented in Australia in 1980 and first incorporated by HEATRIK™ (UK) in a refrigerator in 1985.

The Compact heat exchanger has high area density i.e. heat transfer area to the unit volume of the heat exchanger $\geq 700 \text{ m}^2/\text{m}^3$, hydraulic diameter $D_h = 6 \text{ mm}$ gas to gas

applications and $\geq 400 \text{ m}^2/\text{m}^3$ for liquid to gas applications. Whereas the area density of printed circuit heat exchanger is $\geq 2500 \text{ m}^2/\text{m}^3$. Because of the compactness as well as high performance ($\epsilon > 0.90$), the demand of PCHE is increasing for volume limited cryogenic application.

PCHEs are constructed from flat metal plates on which fluid flow channels are chemically etched. The chemical etching technique is similar to that employed for etching electrical printed circuits hence is capable of producing fluid circuits of unlimited variety and complexity configuration.

The required configuration of the channels on the plates for each fluid is governed by the temperature and pressure drop constraints for the heat exchange duty. Once an optimal thermal design has been developed for an exchange, the artwork required for plate manufacture is quickly and conveniently computer-generated.

1.1.1. Advantages of PCHE:

- ❖ Flow of fluid in microchannels are optimized for counter flow
- ❖ Area density (heat transfer area per unit volume) is very large $\geq 2500 \text{ m}^2/\text{m}^3$
- ❖ PCHE can operate high range of pressure up to 600bar and temperature ranges from cryogenic temperature from -200 to 900°C
- ❖ High heat transfer coefficient is obtained due to small hydraulic diameter.
- ❖ Due to high compact design size is 4 to 6 times smaller than the conventional heat exchanger.
- ❖ PCHE are applicable for gases, liquids and also two-phase flows
- ❖ High performance effectiveness greater than 0.90 ($\epsilon > 0.90$)

1.1.2. Disadvantages of PCHE:

- ❖ PCHE is very expensive as compared to conventional heat exchangers.
- ❖ Fluids should be extremely clean to avoid contamination.
- ❖ Due to small size ($D_h \leq 1\text{mm}$) blockage can occur.
- ❖ Filters required cleaning regularly.

1.1.3. Materials Selection

Material selection for PCHE depends on the following parameters

- ❖ low density
- ❖ high thermal conductivity
- ❖ have high strength and ductility at low temperature up to 4K
- ❖ low weight

Materials commonly used in PCHE is austenite stainless steel, alloys, titanium and nickel (pure/alloy). Carbon steel is not used because due to small channel hydraulic diameter zero corrosion allowance to avoid channel blockage. And also carbon steel is not suitable for diffusion bonding.

Materials available

- ❖ Stainless steel 316L/316,304L/304
- ❖ Duplex 2205
- ❖ Titanium grade 2
- ❖ 6moly (NO 8367)

Material development


- ❖ Alloy 59 (NO 6059)
- ❖ SS310 (S31008)
- ❖ 800H(NO 8810)
- ❖ Alloy 617
- ❖ Dual material (copper to stainless steel)

1.1.4. Manufacturing

The development of printed circuit heat exchanger is achieved with innovative manufacturing technology;

(1) Chemical etching and (2) Diffusion bonding

The flow channels of printed circuit heat exchanger are constructed by chemical etching on metal plates in various configurations. Plates are then stacked and assembled by diffusion bonding. The required configuration of the channels, on the plates for each fluid governed by the temperature and pressure constraints for the heat exchanger duty. The design of channel on plates is manufactured conventionally, and quickly computer generated.

Chemical etching + diffusion bonding  PCHE

Fabrication steps:

Plates  chemical etching  stacking  diffusion bonding  PCHE

1.1.5. Design of Printed Circuit Heat Exchanger (HEATRIC™ type)

The Heatric™ is a printed circuit heat exchanger with area density greater than $\geq 2500 \text{ m}^2/\text{m}^3$. The name originated from its manufacturing process; the fluid passages are photochemically etched.

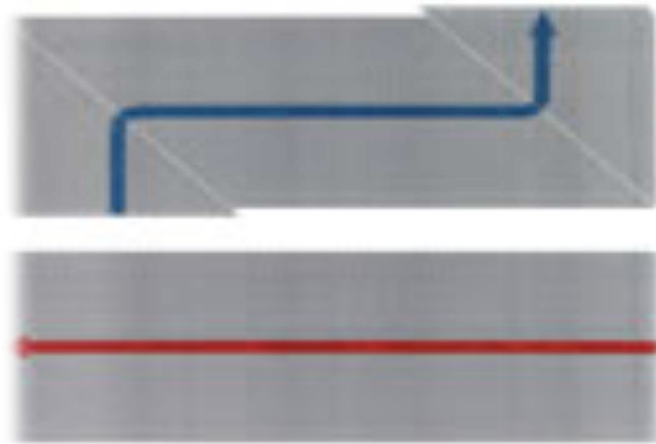


Figure 1.1. Step 1. Plate passage [1]

The metal plates assembled and joined by diffusion bonding. Due to diffusion bonding the lifetime of the heat exchanger is longer than any heat exchanger based on brazed structure.

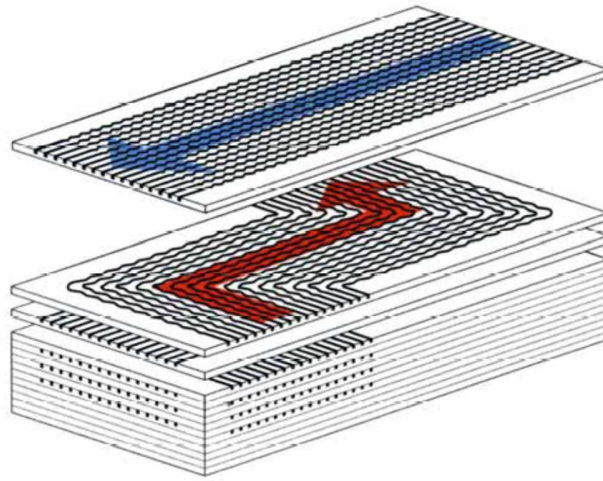


Figure 1.2. Step 2. Diffusion bonding of plates [1]

A stacked of etched plates bonded together and forms a block. A complete heat exchanger core is composed of by welding together number of these blocks as requirement according to the thermal duty of heat exchanger (Figure 1.3).

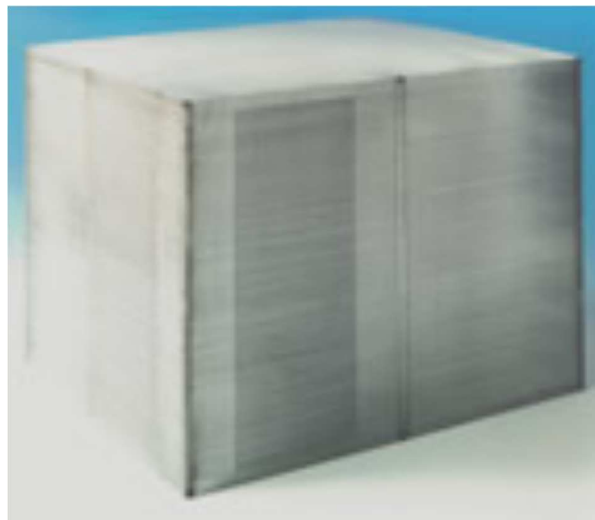


Figure 1.3 Step 3. A blocked composed of diffusion bonded plates [1]

Fluid nozzles and headers are welded directly into the core Fig. 1.4,. The flow passages are typically semi-circular cross section and the width varies from 1.0 mm to 2 mm, depth varies from 0.5 mm-1.0 mm.



Figure1.4.Step 3 welding of nozzles and header to Heat exchanger [1]



Figure1.5.The final Product [1]

Their weight prices HEATRIC™. HEATRI™ heat exchangers are capable to operate up to 60 Mpa and temperature from cryogenic to high temperature 900°C. The material used in PCHE are austenite stainless steel, nickel, and titanium because of corrosion resistant. Use of Carbon steel is provided due to two reasons first is carbon steel is not

applicable for diffusion bonding. Second is HEATRIC™ are designed free from corrosion resistant so as the channel diameter is small to avoid passages blockage. Heatric™ has no brazed material and gaskets. Leakage of fluid is reduced due to continuous passages. The micro-channel design prevents vibrational damage and tube rupture. The most advantage of HEATRIC™ is free from fouling for gas to the gas application. HEATRI™ Heat exchangers are versatile one applicable for liquid, gases, two-phase flow (boiling and condensing) and also design for multi-stream capacity. The most employed flow arrangements are counter flow and cross flow.

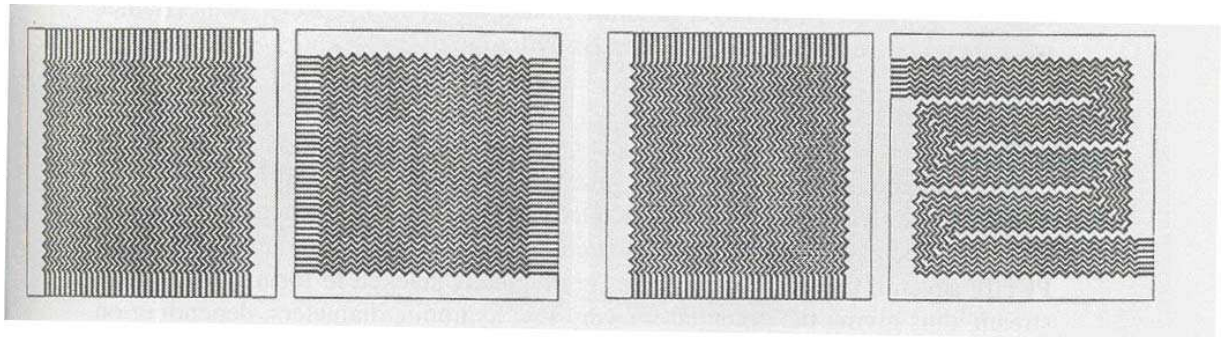


Figure 1.6. Simple cross flow (left) and cross flow (right) configuration [2]

1.1.6. Applications

Hydrocarbon gas and NGL processing

- Gas –Gas Exchanger
- Gas dehydration
- Gas compression
- LNG, LPG, synthetic fuel production

Chemical Processing

- Pharmaceuticals
- Ammonia, Methanol, Acids
- Chlorine, Formaldehyde

Refining

- Air separator
- Power and energy

- Chillers and condensers
- Cascade condensers
- Absorption cycles
- Geothermal generation
- Nuclear application
- Reactor feed

1.2. Axial conduction

The axial conduction problem appears when there is a large temperature difference exists in a single heat exchanger and when both the fluid flowing through the heat exchanger has same specific heat. Due to small size compact heat exchangers have large temperature gradient than the conventional heat exchanger. The effect of axial conduction cannot be negligible. Axial conduction is described as a dimensionless parameter λ .

To describe axial conduction or back conduction let's consider laminar fluid flow through a circular duct and subjected to constant heat flux boundary condition on its surface. Heat applied to the outer surface flows in the radial direction along the solid wall using conduction. When it reaches the solid-fluid interface, the heat flows into the water and get carried out with the flow of fluid in the forward direction. So the bulk fluid temperature increases linearly beyond the thermally developing zone i.e. in the fully developed zone. The phenomenon represented in Figure 1.7. The wall temperature also increases linearly in the forward direction hence heat transfer caused in the back direction from high temperature to low temperature at constant heat transfer coefficient. This phenomenon is called as axial conduction or back conduction.

$$q'' = h(T_w - T_s) \quad (1.2)$$

$$T_w = \frac{q''}{h} + T_s \quad (1.3)$$

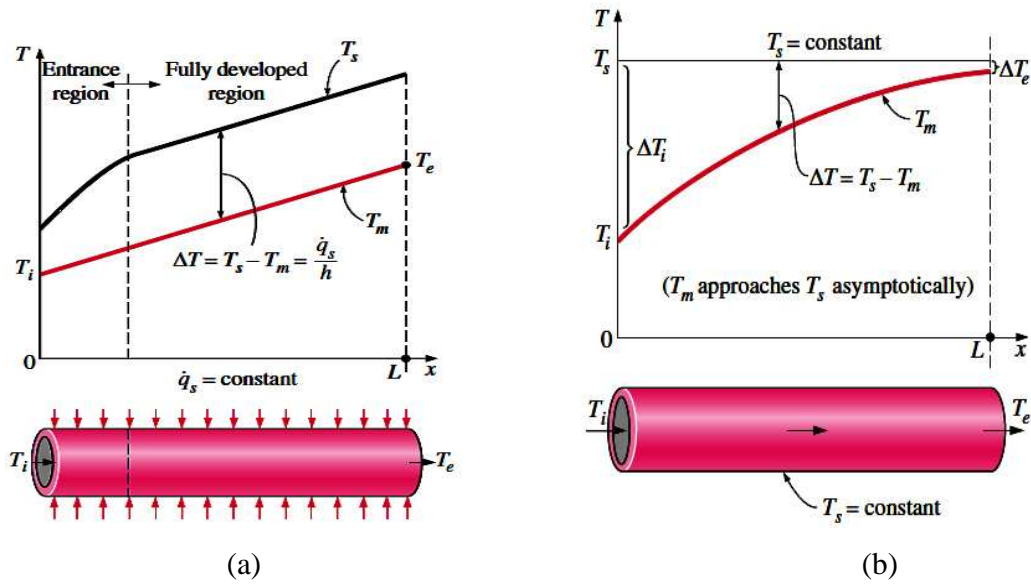


Figure 1.7 Axial variation of bulk fluid and local wall temperature along the flow direction of a circular duct subjected to (a) constant wall heat flux (b) constant wall temperature [3].

When the outer surface circular duct is subjected to constant uniform temperature then it is called as constant wall temperature boundary condition. The bulk temperature variation is not linear and approaches to wall temperature.

Figure (1.7) (a), (b) shows constant heat flux and constant wall temperature boundary condition is applied to the outer surface of the circular duct with specific wall thickness. T_w in Eq. (1.2) or (1.3) represents the solid-fluid interface temperature. It is found that there is a temperature difference along the axial direction and maximum temperature difference at inlet or outlet. In Fig. (1.7) (a), It is observed that there is no temperature gradient along an axial direction at constant boundary condition. So there is no axial heat conduction.

1.3. Objectives of the thesis

The objective of the present work is evolution of the thermal performance of the counter flow rectangular microchannel of PCHE

- ❖ Design and simulation of a 3D rectangular counter flow microchannel (PCHE) by using ANSYS FLUENT15
- ❖ Evaluation of dimensionless form of fluid and wall temperature, heat flux, Nusselt number varying Reynolds number (Re) and wall ratio solid to fluid (k_{sf})
- ❖ Comparison of the Nusselt number heat flux, a dimensionless form of fluid temperature and wall temperature at different Reynolds number.
- ❖ Determination of thermal performance (effectiveness) and axial conduction of the microchannel heat exchanger.

1.4. Organization of thesis

The thesis is organized into five chapters as followings:

Chapter 1 describes the introduction of printed circuit heat exchanger (PCHE), PCHE material selection, manufacturing, advantages and disadvantages, flow arrangement. The objective of the thesis is highlighted.

Chapter 2 is the literature review of Printed circuit heat exchanger and as well as microchannel.

Chapter 3 covers the numerical analysis of a three dimensional rectangular counter flow microchannel using CFD FLUENT.

Chapter 4 covers the results and discussion.

Chapter 5 makes the conclusion of this thesis.

References

CHAPTER 2

Literature review

2.1 Microchannel

Microchannel was developed by Tuckerman and Pease in 1980 at Stanford University.

Tuckerman and Pease [4] had introduced the concept of microchannel. The demonstration was done in microchannel sink that chips could be cooled by forced convective water through microchannels. A rectangular microchannel (silicon) was fabricated with width 50 microns and depth of 302 microns. It was capable to dissipate 790W/cm^2 . Found the temperature of the substrate raised to 71°C , which is above the inlet temperature of the water.

Ravigururajan et al. [5] investigated experimentally to study the characteristics of a parallel microchannel in a single phase. Refrigerant-124 was used as working fluid, and the mass flow rate varied from 35 ml/min to 300 ml/min. The heat flux varied from 10 W/cm to 100 W/cm. The result found that the heat transfer coefficient increased by 20%.

Hasan et al. [6] made a counter flow 3D microchannel heat exchanger of various geometries to investigate the thermal and hydraulic performance numerically. The performance is observed for different channel cross sections circular, square, rectangular, iso-triangular, and trapezoid. Found for the same volume as the number of the channel increased the effectiveness increased. The circular channel gave the best performance.

Moharana et al. [7] had done a numerical study to determine the effect axial conduction in a rectangular microchannel developing laminar flow. The bottom surface was at constant heat flux boundary condition; other surfaces are insulated. The numerical simulation had done for a range of k_{sf} 0.17 to 703 and δ_{sf} ranged from 1 to 24 and Reynolds number from 100 to 1000. Result found higher k_{sf} increased the effect of axial conduction, decreased the average Nusselt number.

Moharana et al. [8] had studied the effect of axial conduction on a microtube in the conjugate heat transfer condition. The fluid flow through the tube is laminar and the surfaces in adiabatic condition. Both the cases for constant wall temperature and constant wall heat flux were considered for investigation. The simulation was done by varying k_{sf} i.e. ratio of microtube thickness to inner radius. Result found for constant heat wall flux case there was an optimum k_{sf} at which Nusselt number throughout the microtube is maximum. In second case for constant wall temperature there was no optimum k_{sf} value at which Nusselt number was maximum. The Nusselt number was increasing with increase of k_{sf} and high Nusselt number achieved with thick wall.

Moharana et al. [9] had developed a three dimensional ($0.6 \text{ mm} \times 0.4 \text{ mm} \times 60 \text{ mm}$) substrate with the microchannel. The aspect ratio varied from 0.45 to 4. The effect of axial conduction is noticed at low Reynolds number; Reynolds number kept constant at 100. Constant heat is applied to the bottom surface while other surfaces are insulated. The thermal conductivity of the solid substrate and the fluid are taken in the conjugate formulation. The local Nusselt number and average Nusselt number are found as varies with the aspect ratio.

Moharana et al. [10] had done a numerical analysis to define the effect of axial conduction on a two dimensional partially heated microtube of inner radius 0.2mm and 60mm length in conjugate heat transfer condition. The fluid flow through the microtube was laminar. 6 mm at both inlet and outlet of microtube was insulated and rest 48 mm length was subjected to constant wall temperature boundary condition. The cross sectional surfaces of solid subjected to adiabatic wall. The simulation was done on varying wide range of ratio of thermal conductivity solid to fluid (k_{sf}), ratio of solid wall thickness to fluid wall thickness (δ_{sf}) and Reynolds number (Re) as described above and also fully heated microtube case. Result found for case of fully heated microtube that the average Nusselt (Nu_{avg}) number was increased with the decrease of wall conductivity. Thicker wall had high average Nusselt number (Nu_{avg}). In case of partially heated microtube the average Nusselt number for thicker wall was less as compared to the thinner wall microtube. The average Nusselt number was high as compared to thin wall microtube at low wall conductivity.

Moharana et al. [11] had investigated numerically the effect of axial conduction on the thermal performance of a microtube at cryogenic temperature. The microtube was subjected to constant heat flux and the surfaces were insulated. The thermo-physical properties as a function of temperature were taken for the analysis. Simulation was done on varying Reynolds number, k_{sf} , thermal conductivity ratio and δ_{sk} , ratio of microtube wall thickness to the inner radius of the microtube. Result found average Nusselt number (Nu_{avg}) lower for higher wall thickness of microtube.

2.2 Printed circuit heat exchanger

The use of the microchannel in heat exchanger has been known for the decade; HEATRICTH produced the first unit in 1985. One company HEATRICTM [1] has fabricated channel of heat exchangers. The only reference HEATRICTM is Hessel greaves compact heat exchanger published in 2001 [2].

Kim et al. [12] performed a numerical analysis on a three dimensional zig-zag channel printed circuit heat exchanger model to investigate characteristics of heat transfer and pressure drop of a supercritical CO₂. The validation was compared with the previous experimental data and found numerical data was deviated 10% from the experimental data. A new PCHE airfoil model was designed. On comparison found that area density was same with the zig-zag channel and in case of pressure drop it was reduced to one-twentieth of the zig-zag channel.

Tsuzuki et al. [13] had done a three dimensional simulation of an s-shape channel and sine curve channel printed circuit heat exchanger recuperators of CO₂. Found the result as at the same thermal performance the new configuration s-shape and sine shape channel configuration had one-fifth pressure drop as compared to the zig-zag channel.

Mylavarapu et al. [14] had done an investigation on various high temperatures up to 900°C and pressure up to 3 Mpa. High-temperature helium test facility was for validation. Result found that alloy 617 and 230 are most leading material for high-temperature PCHE. Two PCHE are fabricated from alloy 617 each having ten hot plates and ten cold plates with 12 flow channels in each plate. Two PCHE are tested in the helium test ring. CFD calculation also is done for three different flow rates of 15, 40, 80 kg/h at 3 Mpa pressure. High-temperature materials, the design of helium

test facility, the design and fabrication of printed circuit heat exchanger are focused in the CFD study.

Kim et al. [15] developed a printed circuit heat exchanger having longitudinal corrugation flow channels to evaluate the hydraulic performance in low Reynolds number region ($Re \leq 150$). The validation is compared with the measured data obtained experimentally. Data demonstrated with helium gas. The numerical results fairly good compared to experimental data.

Kim et al. [16] investigated both numerically and experimentally the hydraulic and thermal performance of a printed circuit heat exchanger in a helium water condition with vertical and horizontal settings. The numerical simulation was validated with experimental data. Numerical simulation was done to the Reynolds number 2500. The results were that the fanning factor of helium and water range was less than 0.97% and 0.66%.

Baek et al. [17] had done the experimental investigation to determine the thermal and hydraulic performance of a PCHE with multiple corrugated longitudinal microchannels working under cryogenic temperature. Thermal performance is affected by axial conduction in low Reynolds number. To increase the effectiveness the design of PCHE was modified to reduce the axial conduction.

Baek et al. [18] designed three PCHE, first heat exchanger, is conventional type, second heat exchanger has modified cross section to reduce longitudinal conduction and third heat exchanger is modified in cross section and in cross link in parallel channels to reduce flow maldistribution. All three PCHE were tested under cryogenic single phase and two phase environments both experimentally and numerically. Found that the first PCHE showed ideal thermal performance whereas in other two PCHE the thermal performance is affected by axial conduction and fluid flow maldistribution.

Lee et al. [19] analysed the effect of the geometric parameter on the performance of a three dimensional PCHE. The numerical value was validated with the available experimental value. The effect of design parameters i.e. channels angle and semi-elliptical aspect ratio on the performance of heat transfer and friction in the cold channel was determined

CHAPTER 3

Numerical simulation

3.1 Introduction

While considering heat transfer in the microchannel heat exchanger, axial conduction is found a potential problem at low Reynolds number in cryogenic temperature range. Effect of axial conduction plays a role in the longitudinal direction.

In this project work, a three dimensional analysis is carried out and studied the effect of axial conduction on conjugate heat transfer in the cryogenic microchannel heat exchanger. The microchannel heat exchanger's outer surface is in adiabatic condition. A three dimensional rectangular micro-channel heat exchanger ($40\text{ mm} \times 1.2\text{ mm} \times 0.8\text{ mm}$) is designed. The microchannel has a single hot fluid flow channel and a single cold fluid flow channel ($40\text{ mm} \times 0.4\text{ mm} \times 0.2\text{ mm}$).

The computational domain consists of three sub-domain i.e. (a) the hot channels (b) cold channels and (c) steel separators. Fluid flow channel plates are arranged alternately using a separator. The convective heat transfer in the cold and hot channels and heat conduction in the separators are calculated in the domains.

In this chapter, the fundamental governing equations (continuity, momentum, energy equations) are implemented which are derived from basic principles of heat and fluid flow.

3.2 Governing equations

Numerical Analysis is performed using the commercially available ANSYS FLUENT. The governing equation for 3-D steady laminar flow and conjugate heat transfer in rectangular counter flow microchannel printed circuit heat exchanger has been modelled and simulated numerically.

Steady state continuity, momentum (Navier-Stokes equation) and energy equation are determined in laminar and compressible flow.

Conservation of mass (Continuity equation):

$$\frac{\partial u}{\partial x} + \frac{\partial v}{\partial y} + \frac{\partial w}{\partial z} = 0 \quad (3.1)$$

Conservation of momentum equation in x, y, z directions (Navier-Stokes equation)

$$\rho \left(u \frac{\partial u}{\partial x} + v \frac{\partial u}{\partial y} + w \frac{\partial u}{\partial z} \right) = -\frac{\partial p}{\partial x} + \mu \left(\frac{\partial^2 u}{\partial x^2} + \frac{\partial^2 u}{\partial y^2} + \frac{\partial^2 u}{\partial z^2} \right) \quad (3.2)$$

$$\rho \left(u \frac{\partial v}{\partial x} + v \frac{\partial v}{\partial y} + w \frac{\partial v}{\partial z} \right) = -\frac{\partial p}{\partial y} + \mu \left(\frac{\partial^2 v}{\partial x^2} + \frac{\partial^2 v}{\partial y^2} + \frac{\partial^2 v}{\partial z^2} \right) \quad (3.3)$$

$$\rho \left(u \frac{\partial w}{\partial x} + v \frac{\partial w}{\partial y} + w \frac{\partial w}{\partial z} \right) = -\frac{\partial p}{\partial z} + \mu \left(\frac{\partial^2 w}{\partial x^2} + \frac{\partial^2 w}{\partial y^2} + \frac{\partial^2 w}{\partial z^2} \right) \quad (3.4)$$

Conservation of energy equation

$$\begin{aligned} \rho c_p \left(u \frac{\partial T}{\partial x} + v \frac{\partial T}{\partial y} + w \frac{\partial T}{\partial z} \right) = k \left\{ \frac{\partial^2 T}{\partial x^2} + \frac{\partial^2 T}{\partial y^2} + \frac{\partial^2 T}{\partial z^2} \right\} + \\ 2\mu \left\{ \left(\frac{\partial u}{\partial x} \right)^2 + \left(\frac{\partial v}{\partial y} \right)^2 + \left(\frac{\partial w}{\partial z} \right)^2 \right\} + \mu \left\{ \left(\frac{\partial u}{\partial y} + \frac{\partial v}{\partial x} \right)^2 + \left(\frac{\partial u}{\partial z} + \frac{\partial w}{\partial x} \right)^2 + \left(\frac{\partial v}{\partial z} + \frac{\partial w}{\partial y} \right)^2 \right\} \end{aligned} \quad (3.5)$$

Assumptions used in PCHE modelling

- A steady state condition is to be assumed.
- Assumed to be a uniform flow.
- The density of helium along the flow path changes.
- The outer surface of the metal plates i.e. makes the PCHE are assumed adiabatic wall.
- Laminar flow $Re \leq 100$.
- Pressure drop is negligible.
- Specific heat of helium (C_p) remains constant.

3.3 Selection of materials

The thermo-physical properties of the material are independent of temperature. For simulation, the following metals listed below from $k_{sf} = 141.58$ to 5061.5 are used in this work.

Table 3.1 List of materials used for the microchannel

Sl.No.	Materials	Density ρ (kg/m ³)	Specific heat C_p (J/kg- K)	Thermal conductivity of solid k_s (W/m-K)	Thermal conductivity of fluid k_f (W/m-K)	$k_{sf} =$ k_s/k_f
1	Nichrome	8400	420	12	0.08672	141.58
2	SS 316	8238	468	13.4	0.08672	158.09
3	Constantan	8920	384	23	0.08672	271.36
4	Chromium steel	7822	444	37.7	0.08672	444.79
5	Nickel	8900	460	91.74	0.08672	1082.38
6	Alloy 195	2790	883	168	0.08672	1982.12
7	Silver	10500	235	429	0.08672	5061.5

3.4 Thermo-physical properties of cryogenic fluid

In cryogenic temperature, the thermo-physical properties are very sensitive. For a very small variation of temperature, property changes appreciably. The density, viscosity, thermal conductivity and specific heat of Helium are dependent on temperature. But the specific heat is constant with temperature variation. Hence, UDF of thermo-physical properties as a function of temperature is used in simulation process considering the following mentioned mathematical equations for density, thermal conductivity and viscosity [20].

$$\rho_{(T)} = 0.1186 + 3.38334e^{\left[-\frac{T}{20.41}\right]} + 0.93142e^{\left[-\frac{T}{99.36854}\right]} \quad (3.6)$$

$$k_{f(T)} = 0.00793 + 0.000878621T - 2.50172 \times 10^{-6}T^2 + 3.92 \times 10^{-10}T^3 \quad (3.7)$$

$$\mu_{f(T)} = -4.25462 \times 10^{-7} + 8.25786 \times 10^{-8}T - 9.43838 \times 10^{-11}T^2 + 7.6085 \times 10^{-14}T^3 \quad (3.8)$$

Specific heat of helium remains constant in the range of $50 \text{ K} \leq T \leq 300 \text{ K}$ [18], which is approximately equal to 5200 J/kg-K.

3.5 Grid independence test.

Grid independence test is carried out for the square microchannels with zero thickness to check grid size. The entire domain is meshed with rectangular elements, and then the sensitivity is checked to choose the best mesh. Local Nusselt Nu_z for

three different grids of number cells 660825, 897120, 1285284 are determined. The second one is selected as there is no appreciable difference is noticed with the other two.

3.6 Computational domain and boundary condition

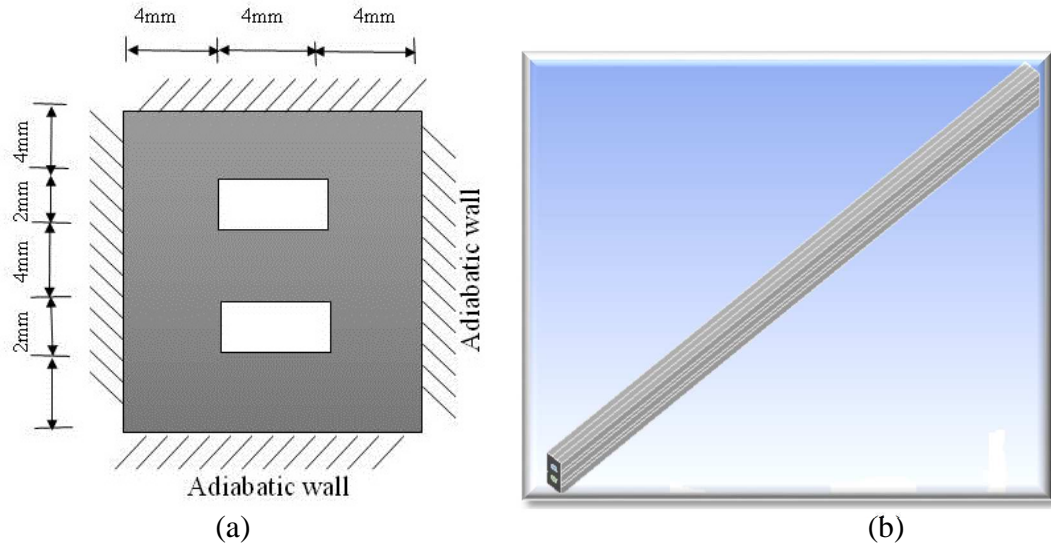


Fig. 3.1. (a) Computational domain, (b) geometry of microchannel heat exchanger.

Table. 3.2 Boundary conditions

Sl. No.	Boundary condition	Laminar flow
1	Velocity inlet	Velocity magnitude, Temperature
2	Pressure outlet	Gauge pressure
3	Wall (outside)	Heat flux = 0
4	Wall (fluid/solid interface)	Thermally coupled wall condition

Table.3.3. Velocity at Reynolds number 50

Properties	Temperature (K)	Mass flow rate (\dot{m} kg/sec)	Velocity (m/sec)
$T_{\text{hot, in}}$	100	0.00010447	2.6964
$T_{\text{cold, in}}$	200	0.000193854	9.9616

Table.3.4. Velocity at Reynolds number 80

Properties	Temperature (K)	Mass flow rate (\dot{m} kg/sec)	Velocity (m/sec)
$T_{\text{hot, in}}$	100	0.000167151	4.3143
$T_{\text{cold, in}}$	200	0.000310166	15.9386

3.7 Mathematical Modelling

Axial conduction (λ):

Longitudinal conduction or axial conduction is determined by a dimensionless parameter λ . According to Kroeger's [21] analytic the dimensionless axial conduction parameter λ is defined with heat exchanger length (L), cross-sectional area of wall (A_w), thermal conductivity of wall (k_w) and heat capacity rate (C) as the following equation

$$\lambda = \frac{k_w A_w}{LC_{\min}} \quad (3.9)$$

where k_w is thermal conductivity of the wall, A_w is cross-sectional area of the wall, L is the length of the heat exchanger and C_{\min} is the heat capacity. To design a compact heat exchanger for cryogenic purpose the axial conduction λ should be low that is controlled by varying the length of heat exchanger and the cross-sectional area.

Effectiveness (ϵ): Effectiveness of a heat exchanger is defined as the ratio of actual heat transfer to the maximum possible heat transfer.

$$\epsilon = \frac{Q_{\text{actual}}}{Q_{\text{max}}} \quad (3.10)$$

$$\epsilon = \frac{C_{p, \text{hot}} (T_{\text{hot, in}} - T_{\text{hot, out}})}{C_{p, \text{min}} (T_{\text{hot, in}} - T_{\text{cold, in}})} \quad (3.11)$$

where $C_{p, \text{min}}$ is equal to $C_{p, \text{hot}}$ or $C_{p, \text{cold}}$. Temperature values are used to calculate the effectiveness of heat exchanger. The specific heat capacity of fluid is assumed to be constant.

Ineffectiveness ($1-\epsilon$): Ineffectiveness is a parameter used to estimate the thermal performance of a heat exchanger. For a counter flow heat exchanger, axial conduction and NTU is used to estimate ineffectiveness.

Local Nusselt number (Nu): Nusselt number is given by the ratio of convection to conduction

$$Nu = \frac{h_{\text{hot}} D_h}{k_{\text{Helium}}} = \frac{h_{\text{cold}} D_h}{k_{\text{Helium}}} \quad (3.12)$$

where D_h is the hydraulic diameter of rectangular microchannel

$$Nu = \frac{h_{hot} D_h}{k_{Helium}} = \frac{h_{cold} D_h}{k_{Helium}} \quad (3.12)$$

$$D_h = \frac{4A_{cs}}{P} \quad (3.13)$$

Local heat transfer coefficient (h):

$$h = \frac{q''}{T_w - T_f} \quad (3.14)$$

Dimensionless form of fluid Temperature

$$\Theta_f = \frac{T_f - T_{fcold,in}}{T_{fhot,in} - T_{fcold,in}} \quad (3.15)$$

Dimensionless form of wall Temperature

$$\Theta_w = \frac{T_w - T_{fcold,in}}{T_{fhot,in} - T_{fcold,in}} \quad (3.16)$$

Reynolds number (Re): It is the ratio of inertia forces to viscous force, Reynolds number is used to identify the flow regions whether laminar or turbulent.

$$Re = \frac{\rho v D_h}{\mu} \quad (3.17)$$

3.8 Solution approaches

Step 1: Hydraulic diameter is calculated

$$D_h = \frac{4A_{cs}}{P} = \frac{4HW}{2(H+W)} \quad (3.18)$$

Step 2: Velocity is calculated by using Reynolds number

$$v = \frac{Re\mu}{\rho D_h} \quad (3.19)$$

Step 3: Mass flow rate is calculated

$$\dot{m} = \rho_f v_f D_h \quad (3.20)$$

CHAPTER 4

Results and discussion

As described in chapter 3 a three dimensional counter flow microchannel heat exchanger domain is simulated to study the effect of axial conduction in the longitudinal direction and the thermal performance of heat exchanger. Both the calculation parameters are investigated with varying different materials and Reynolds number (Re). The surfaces are an adiabatic wall. The interested parameters are wall temperature and fluid temperature, heat flux in conjugate surface and Nusselt number. The flow through the channel is laminar and steady.

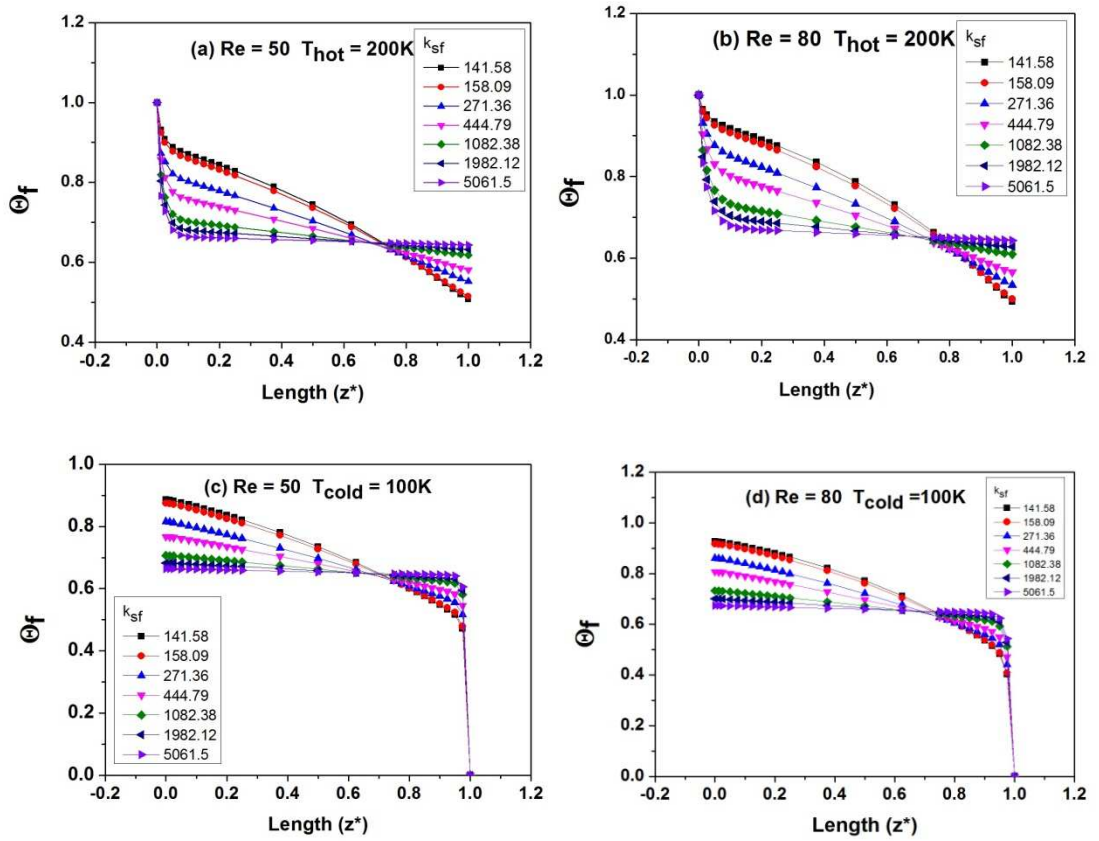


Fig. 4.1. Variation of dimensionless fluid temperature along the length of microchannel heat exchanger as a function of Re and k_{sf} (a-b) hot channel (c-d) cold channel.

Figure. 4.1 (a) (b) represent, the temperature variation of the fluid according to k_{sf} along the length. In between 0.6 to 0.8 there is a transition point. Between 0 to 0.7

temperature decreases according to k_{sf} , deflection is more for low k_{sf} . In between 0.7 to 1.0 temperature curve is low for high k_{sf} .

Figure 4.1 (c) (d) represent the temperature of fluid varies from 1.0 to 0. Here also there is a transition point. Temperature increases in between 0 to 0.7 with the increase of k_{sf} . In between 0.7 to 1.0 low k_{sf} has high temperature whereas high k_{sf} has low temperature variation.

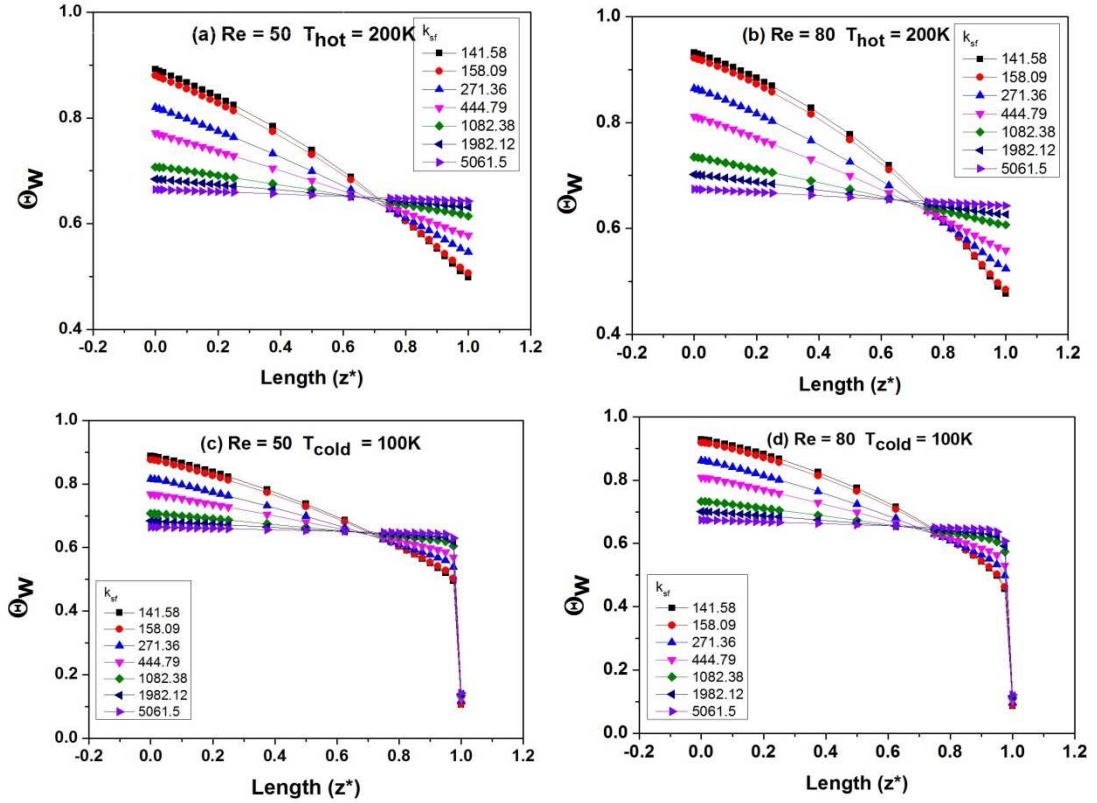


Fig. 4.2. Variation of dimensionless wall temperature along the length of microchannel heat exchanger as a function of Re and k_{sf} (a-b) hot channel (c-d) cold channel.

Wall temperature for hot channel varies linearly (decreases) as shown in Fig. 4.2 (a) (b), along the length according to k_{sf} . Above the transition point, temperature curve is high for low k_{sf} and below the transition point the temperature curve is high for high k_{sf} .

Wall temperature for the cold channel as shown in Fig. 4.2 (c) (d) varies along the length from 1 to 0. The temperature increases with the increase of k_{sf} . Above the transition point, high k_{sf} has low temperature and low k_{sf} has high-temperature

variation is noticed. Below the transition point, low k_{sf} has high temperature variation curve vice versa.

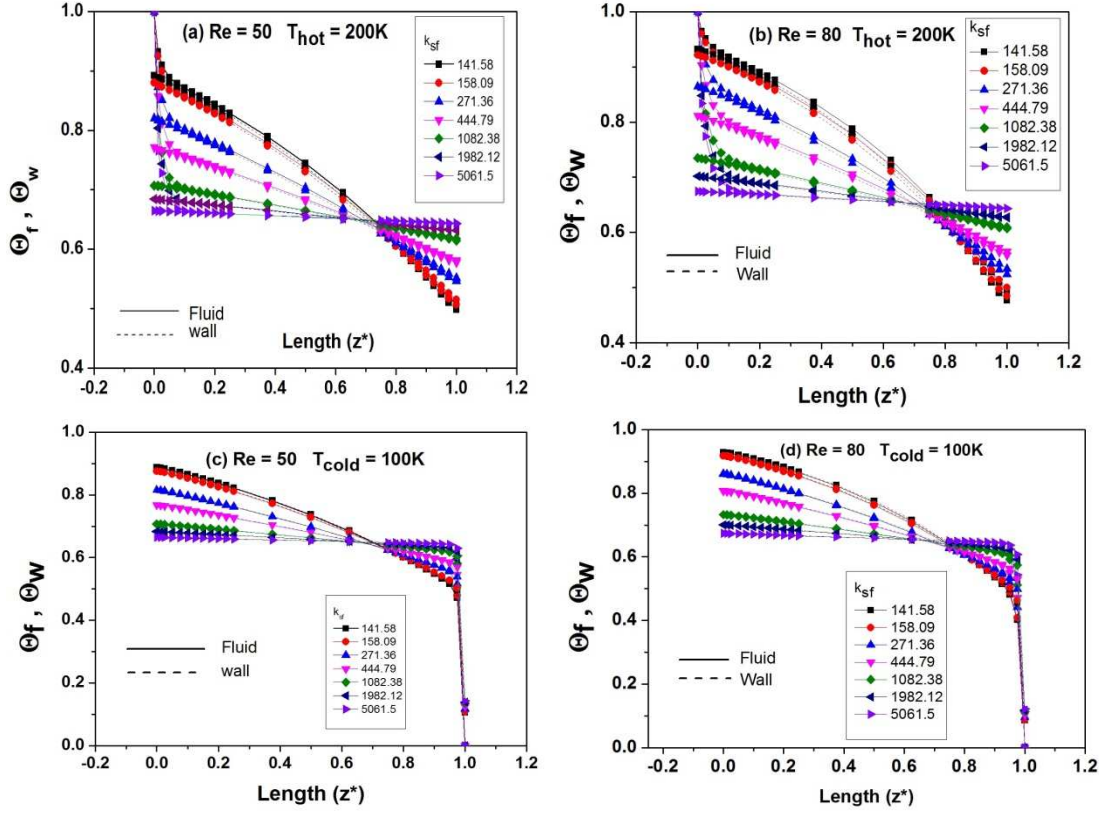


Fig.4.3. Variation of dimensionless wall and fluid temperature along the length of microchannel heat exchanger as a function of Re and k_{sf} (a-b) hot channel (c-d) cold channel.

Figure 4.3 (a), (b) and (c), (d) shows the variation of dimensionless fluid and wall temperature along the length of the hot channel and cold channel respectively as a function of Re and k_{sf} . There is the very small difference is noticed between both the temperature curves i.e. wall and fluid of each case of k_{sf} .

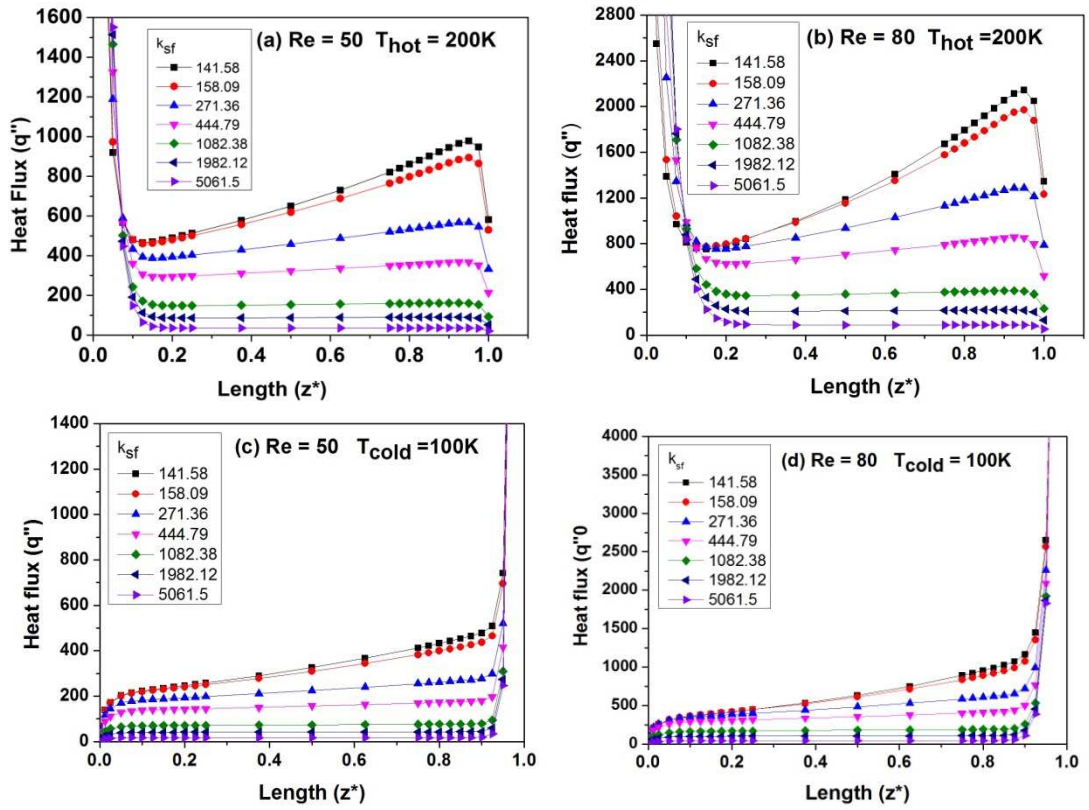


Fig. 4.4. Variation of heat flux along the length of microchannel heat exchanger as a function of Re and k_{sf} (a-b) hot channel (c-d) cold channel.

Heat flux variation for the conjugate surface is increases as shown in Fig. 4.4 (a) (b) along the length of microchannel heat exchanger from 0.1. Conjugate heat transfer for low k_{sf} is high and decreases with the increase of k_{sf} both for $Re = 50$ and $Re = 80$ in the hot channel.

Conjugate heat flux, as shown in Fig. 4.4 (c) (d), varies with k_{sf} . Heat flux is high at the inlet of the cold channel and decreases along the length towards the outlet. Low k_{sf} has high heat flux and decreases with the increase of k_{sf} .

In both hot channel and cold channel ($Re = 50$ and $Re = 80$) heat flux variation is high for low k_{sf} . Heat flux approaches to constant in case of high k_{sf} .

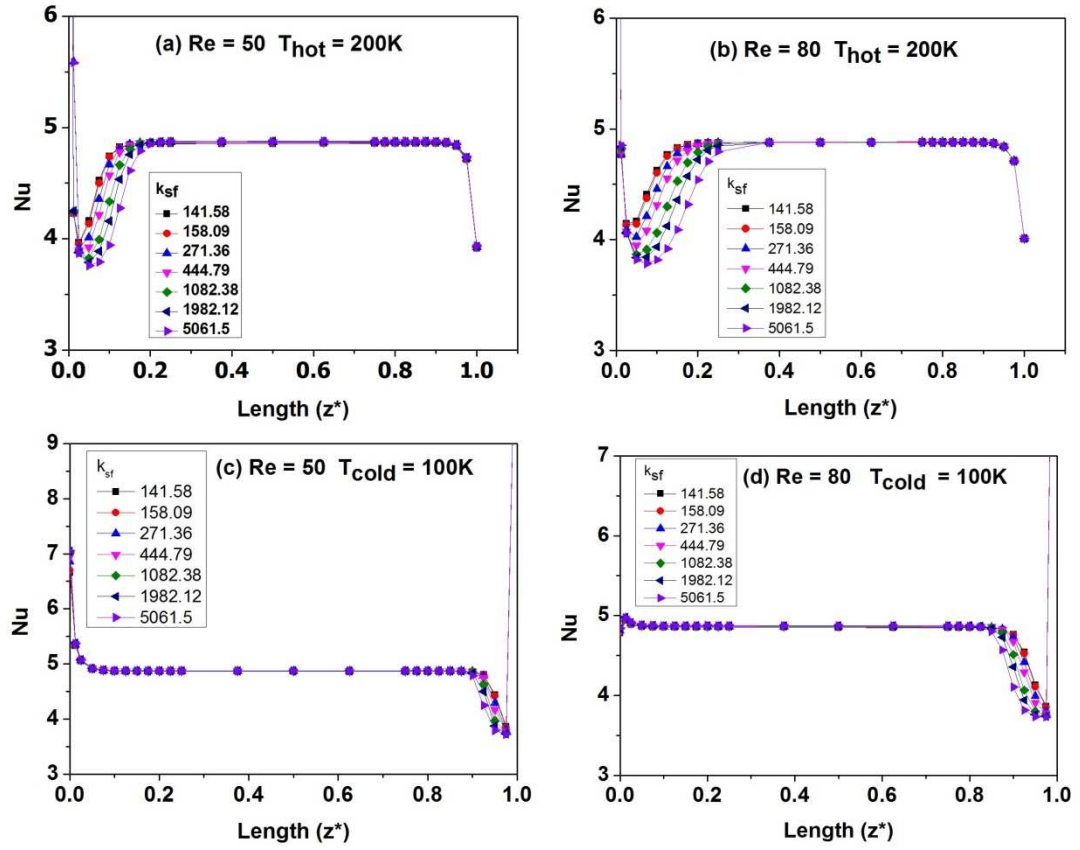


Fig. 4.5. Variation of Nusselt number along the length of microchannel heat exchanger as a function of Re and k_{sf} (a-b) hot channel (c-d) cold channel.

Figure 4.5 (a) (b) shows the variation of Nusselt number in the hot channel at two different Reynolds number $Re = 50$ and $Re = 80$. The Nusselt number is fluctuating in the developing zone from 0.1 to nearly 0.2 with a variation of k_{sf} . The Nusselt number in developed zone remains constant.

Figure 4.5 (c) (d) shows the variation of Nusselt number in the cold channel at two different Reynolds number $Re = 50$ and $Re = 80$. The Nusselt number is fluctuating in the developing zone with a variation of k_{sf} . The Nusselt number in developed zone remains constant.

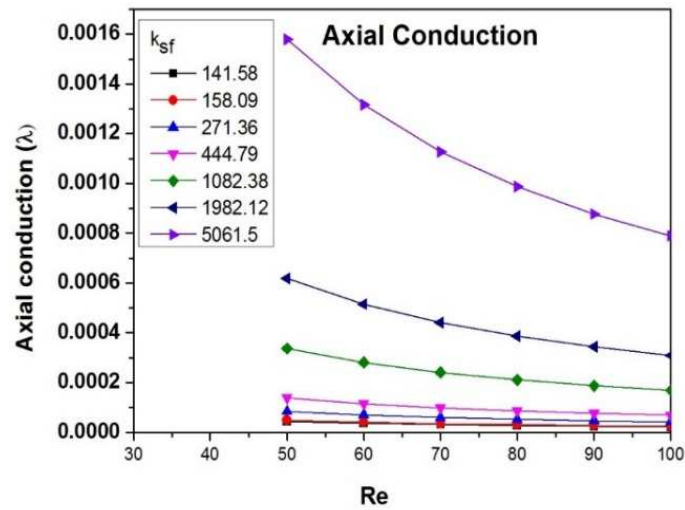


Fig. 4.6. Variation of axial conduction of the microchannel heat exchanger with a variation of Re as a function k_{sf} .

Figure. 4.6. Shows the effect of axial conduction with varying Reynolds number. Axial conduction decreases with the increase of Reynolds number. The effect of axial conduction is high for high k_{sf} and low for low k_{sf} .

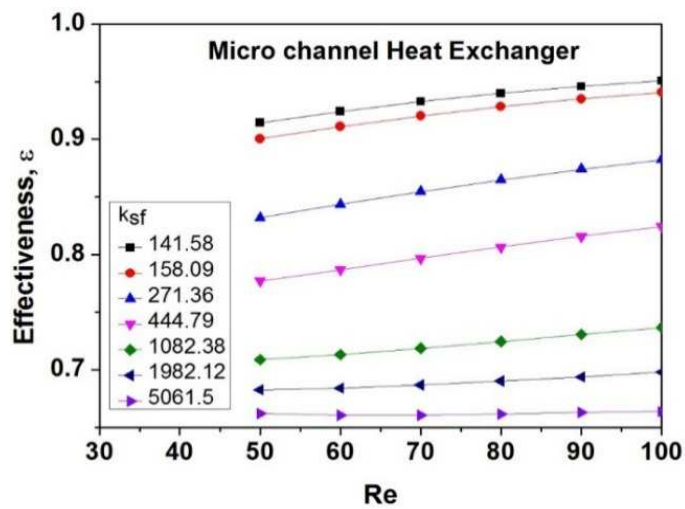


Fig. 4.7. Thermal performance of microchannel heat exchanger (ϵ) with variation of Re as a function of k_{sf}

Low k_{sf} has high effectiveness as shown in Fig. 4.7 and for high k_{sf} effectiveness is low. The effectiveness is also a function of Reynolds number. As Reynolds number increases the effectiveness of the microchannel heat exchanger increase

CHAPTER 5

Conclusion

The fluid flow and the conjugate heat transfer of a rectangular microchannel heat exchanger have been studied successfully using FLUENT under laminar and steady condition.

The calculated parameters are effectiveness, axial conduction, dimensionless fluid temperature, dimensionless wall temperature, and heat flux on the conjugate surface and Nusselt number.

- ❖ The thermal performance of the micro-channel heat exchanger increases with the increase of the Reynolds number. The effectiveness is high ($\epsilon \geq 0.9$) for low k_{sf} , and is lowered with an increase of k_{sf} .
- ❖ The effect of axial conduction is more in low Reynolds number region as the Reynolds number increases the effect of axial conduction diminishes. The axial conduction is high for high k_{sf} and low for low k_{sf} . Low k_{sf} material is preferred where the axial conduction is less for designing high effective microchannel heat exchanger
- ❖ Dimensionless temperature of fluid and wall at different Reynolds number along the length of heat exchanger decreases from inlet to outlet of the hot channel. Temperature of fluid and wall decreases with increasing the k_{sf} .
- ❖ Dimensionless temperature of fluid and wall at different Reynolds number along the length of heat exchanger increases from inlet to outlet of the cold channel. The temperature of fluid and wall increases with lowering k_{sf} .
- ❖ Heat flux on the conjugate surface at different Reynolds number increases along the length of the heat exchanger in the hot channel as a function of k_{sf} . Conjugate heat flux is increasing with lowering the k_{sf}
- ❖ Heat flux on the conjugate surface at different Reynolds number decreases along the length of the heat exchanger in the cold channel is a function of k_{sf} . Conjugate heat flux is decreasing with increasing the k_{sf} .
- ❖ Nusselt number both for hot and cold channel varying in developing zone and remains constant in developed zone.

References

1. Heatic™ Heat Exchanger, <http://www.heatric.com> (Access on 30 May 2015).
2. Hesselgreaves, J.E., Compact Heat Exchangers, Pergamon Press, New York: NY, 2001.
3. Yunus, A. Çengel. "Heat and Mass Transfer." *McGrawHill, New York* (2007).
4. Tuckerman D.B., and Pease R.F., 1981, High-performance heat sinking for VLSI, IEEE Electron Device Letters, IEEE, 2(5), pp. 126-129.
5. Ravigururajan, T. S., Cuta, J., McDonald, C. E., & Drost, M. K. (1996). Single-phase flow thermal performance characteristics of a parallel micro-channel heat exchanger (No. CONF-960815). American Society of Mechanical Engineers, New York, NY (United States).
6. Hasan, M. I., Rageb, A. A., Yaghoubi, M., & Homayoni, H. (2009). Influence of channel geometry on the performance of a counter flow microchannel heat exchanger. *International Journal of Thermal Sciences*, 48(8), 1607-1618
7. Moharana, M. K., & Khandekar, S. (2012). Effect of channel shape on axial back conduction in the solid substrate of microchannels, 3rd European Conference on Microfluidics - Microfluidics 2012 - Heidelberg, December 3-5, 2012.
8. Moharana, M. K., & Khandekar, S. (2012). Numerical study of axial back conduction in microtube, 39th National Conference on Fluid Mechanics and Fluid Power (FMFP2012), 13-15 December 2012, Surat, India.
9. Moharana, M. K., & Khandekar, S. (2013). Effect of the aspect ratio of rectangular microchannels on the axial back conduction in its solid substrate. *International Journal of Micro scale and Nanoscale Thermal and Fluid Transport Phenomena*, 4(3-4), 1-19.
10. Kumar, M., & Moharana, M. K. (2013). Axial Wall Conduction in Partially Heated Microtubes, Proceedings of the 22nd National and 11th International ISHMT-ASME Heat and Mass Transfer Conference, December 28-31, 2013, IIT Kharagpur, India.
11. Yadav, A., Tiwari, N., Moharana, M. K., & Sarangi, S. K. (2014). Axial wall conduction in cryogenic fluid microtube, 5th International and 41st National Conference on Fluid mechanics and Fluid Power (FMFP-2014), 12-14 December 2014, IIT Kanpur, India.

12. Kim, D. E., Kim, M. H., Cha, J. E., & Kim, S. O. (2008). Numerical investigation on thermal-hydraulic performance of new printed circuit heat exchanger model. *Nuclear Engineering and Design*, 238(12), 3269-3276.
13. Tsuzuki, Nobuyoshi, Yasuyoshi Kato, and Takao Ishiduka. "High performance printed circuit heat exchanger." *Applied Thermal Engineering* 27, no. 10 (2007): 1702-1707.
14. Mylavarapu, S., Sun, X., Figley, J., Needler, N., & Christensen, R. (2009). Investigation of high-temperature printed circuit heat exchangers for very high-temperature reactors. *Journal of Engineering for Gas Turbines and Power*, 131(6), 062905.
15. Kim, J. H., Baek, S., Jeong, S., & Jung, J. (2010). Hydraulic performance of a microchannel PCHE. *Applied Thermal Engineering*, 30(14), 2157-2162.
16. Kim, I. H., & No, H. C. (2011). Thermal hydraulic performance analysis of a printed circuit heat exchanger using a helium-water test loop and numerical simulations. *Applied Thermal Engineering*, 31(17), 4064-4073.
17. Baek, S., Kim, J. H., Jeong, S., & Jung, J. (2012). Development of highly effective cryogenic printed circuit heat exchanger (PCHE) with low axial conduction. *Cryogenics*, 52(7), 366-374.
18. Baek, S., Lee, C., & Jeong, S. (2014). Effect of flow maldistribution and axial conduction on compact microchannel heat exchanger. *Cryogenics*, 60, 49-61.
19. Lee, S. M., & Kim, K. Y. (2014). A parametric study of the thermal-hydraulic performance of a zigzag printed circuit heat exchanger. *Heat Transfer Engineering*, 35(13), 1192-1200.
20. Yaws C.L., 1999, Chemical Properties Handbook, McGraw-Hill, New York..
21. Kroeger, P. G. (1967). Performance deterioration in high effectiveness heat exchangers due to axial heat conduction effects. In *Advances in Cryogenic Engineering* (pp. 363-372). Springer US.
22. Shah, Ramesh K., and Dusan P. Sekulic. *Fundamentals of heat exchanger design*. John Wiley & Sons, 2003.